ISSN 0010-5082, Combustion, Explosion, and Shock Waves, 2015, Vol. 51, No. 4, pp. 416–423. © Pleiades Publishing, Ltd., 2015.
Original Russian Text © S.K. Birwa, D.P. Mishra.

Measurements of the Visible Flame Height of a Swirl-Stabilized Kerosene Jet Diffusion Flame

S. K. Birwa[a] and D. P. Mishra[a]

UDC 543.825.3

Published in *Fizika Goreniya i Vzryva*, Vol. 51, No. 4, pp. 20–28, July–August, 2015.
Original article submitted January 21, 2013; revision submitted June 27, 2014.

Abstract: An experimental investigation of the structure of a kerosene-based Jet A1 unconfined flame is conducted for different fuel flow rates and momentum flux ratios (MFRs). A pressure swirl atomizer is used to atomize the fuel jet. It is found that the flame height increases with increasing MFR for a fixed fuel flow rate. However, the flame height first decreased and then increased with increasing fuel flow rate for a fixed MFR. A correlation of the flame height with the power level and MFR is developed in a dimensionless form by using the response surface optimal design method. Variations in the lean blowout limit with the fuel flow rate are also studied. The lean blowout limit first increases to a peak value and then subsequently decreases, in agreement with the behavior of the flame height at the lean blowout limit. A blue region at the top of the flame is observed for high fuel flow rates. The flame characteristics obtained in the study are explained with the help of the spray characteristics of the kerosene fuel.

Keywords: kerosene, spray combustion, design of experiments, momentum flux ratio, pressure swirl atomizer.

DOI: 10.1134/S0010508215040036

INTRODUCTION

Liquid fuel combustors in jet–diesel–oil engines use spray combustion as these liquid fuels have high energy density and are easily transportable. In all such devices, a high-pressure fuel is injected through an atomizer into the combustion chamber. This results in the formation of a spray that helps in faster evaporation leading to better combustion of the fuel. Of all such fuels, the aviation turbine fuel (ATF) is used profusely in aerospace industries due to its higher energy density and customized properties for aircraft engines. Thus, it becomes necessary to determine the flame characteristics of kerosene. The study of the flame height helps in determining the extent of combustion and assessing the heat losses, extent of burning of fuel, emission level, etc. In addition, the combustor length would be dictated by the shape and size of the flame. Hence, experiments were conducted [1–7] to understand the nature of the spray flame. Chigier et al. [1] were among the first researchers who conducted spray flame experiments with a twin fluid atomizer. They performed experiments on an unconfined kerosene spray flame and concluded that spray flames are similar to gaseous jet diffusion flames. Onuma and Ogasawara [2] and Mellor [3] tried to validate this hypothesis. Bracco [8] used the results obtained from single droplet burning tests to predict the spray flame. Assumptions were made that heat is transferred by conduction from the flame to the drop surface and vapor diffuses by molecular diffusion from the drop surface to the flame front [9]. Mellor [10] conducted a series of experiments in a gas turbine test combustor and concluded that a transition from droplet diffusion flames to pure evaporation flames takes place at $\Delta p = 15$ atm. One of the first numerical spray ignition investigations based on a two-phase transient analysis was conducted by Aggarwal and Sirignano [11]. An important aspect revealed from that study was that the spray ignition process is stochastic in nature.

[a]Department of Aerospace Engineering, Indian Institute of Technology, Kanpur, 208016 India; mishra@iitk.ac.in.

The airflow pattern in the primary flame zone is an important factor in flame stability. A common approach is to impart the swirl to the inlet air flow for this purpose. In a swirl-stabilized flame, the fuel jet passes through a strong toroidal vortex [12, 13], which is termed as a recirculation zone. Hence, similar to a bluff body, the swirl creates stagnation points that act as flame holders [14]. This increases the residence time during which the fuel, air, and hot products can coexist [15]. This enhances evaporation of fuel droplets and enables better mixing of the fuel and air. For characterizing the amount of rotation imparted to the axial flow, Beer and Chigier [16] proposed the usage of a dimensionless parameter called the swirl number (SN) [17]:

$$S_N = \frac{2G_m}{G_T D_{\text{sw}}}. \tag{1}$$

Here G_m is the axial flux of the tangential momentum, G_T is the axial thrust, and D_{sw} is the outer diameter of the swirler.

Although the flame height is used to characterize the diffusion flames in the literature, it cannot be considered as an analogous parameter for the flame speed in premixed cases. Gas diffusion flames were characterized earlier in terms of the flame height in several works [4, 18]; also, a few correlations were provided in this respect [5–7, 19]. Shuen [20] tried to explain the effects of the inlet swirl strength and droplet size on the spray flame structure. A strong swirl was found to reduce the flame height owing to improved mixing. Morcos and Abdel-Rahim [21] conducted an extensive study on the effects of the burner geometry and other parameters on the height of confined low-pressure flames of light fuel oil. Nakamura et al. [22] studied the characteristics of kerosene-oxygen spray flames at different pressures and found that the flame height decreases with an increase in the ambient pressure.

The study of the blowout limit is also of great importance because it helps in choosing an optimum lean mixture, reducing hazardous emissions, and producing a desired amount of heat or power. A proper estimate of flame stability can also be obtained. A thorough study on the variation of the flame height and blowout limit of an unconfined Jet A1 flame still remains untouched. The present study explores variations of the flame height with the fuel flow rate and momentum flux ratio. A correlation is proposed for the flame height ratio with the power ratio and momentum flux ratio. In addition, the change in the blowout limit with respect to the fuel flow rate is also studied. In order to accomplish this, an attempt is made to study the flame height just below the threshold blowout limit.

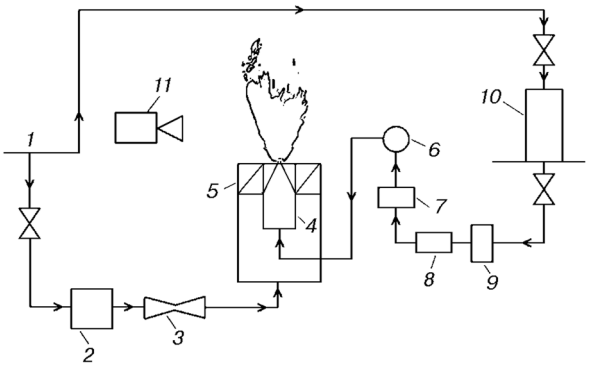

Fig. 1. Experimental setup: (*1*) air from the compressor; (*2*) filter; (*3*) Venturi meter; (*4*) atomizer; (*5*) swirler; (*6*) solenoid valve; (*7*) volume flow meter; (*8*) secondary filter; (*9*) primary filter; (*10*) pressurized fuel tank; (*11*) camera.

1. EXPERIMENTAL DETAILS

Figure 1 shows the experimental setup used for the present combustion study. A pressure swirl atomizer was used for the fuel, and air was passed through a swirler (see Fig. 2). The flame shapes and structures were observed by using a CASIO EXILIM EX-F1 camera.

The fuel used for this study was the Jet A1 (kerosene) fuel obtained from Indian Oil. The 6-liter fuel tank capacity was pressurized with compressed air for supplying the liquid fuel to the atomizer. Two-way filtration was carried out to remove different-sized impurities from the fuel and prevent atomizer blockage. First, the fuel was passed through a combination of fine nets to remove bigger impurities, after which it went through a 15-μm filter for final filtration. The fuel flow rate was measured with a digital flow meter (114 FLO-METER, Range 5H, McMillan Company). Its allowable working range is 50–500 ml/min. The fuel was then passed through a solenoid pump, which enabled us to turn fuel supply on and off according to the requirement.

In order to eliminate any fluctuations in the air flow, a settling chamber upstream of the air supply line was used. The mass flow rate of air was metered with the help of a Venturi meter, which was connected to a U-type differential manometer filled with distilled water. The Venturi meter was calibrated to an average error of 2% at a 95% confidence level in the mass flow rate range from 5.3 to 22.5 g/s.

The pressure swirl atomizer used in this study had a discharge orifice diameter $d_0 = 0.3$ mm (Fig. 2). The diameter was chosen to ensure better atomization. Other parameters were same as in the previ-

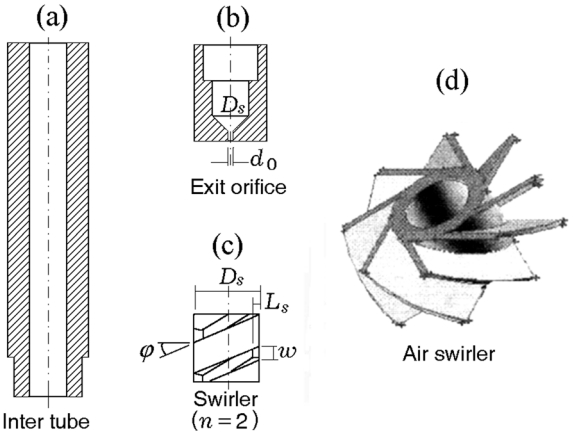

Fig. 2. Pressure swirl atomizer (a and b); swirler with two inlet ports (c); air swirler (d); $S_{N,a} = 0.67$.

ous study [23]. The length to diameter ratio (L_0/d_0) was 1.25. A helical insert was used to impart the swirl motion to the fuel flow [23]. Both the swirler diameter D_s and length L_s were 5 mm. The insert had two ports ($n = 2$) with a cross-sectional area $w \times l = 0.65$ mm^2 and a turn angle $\varphi = 23°$. The swirl imparted to the fuel flow depends on the size of this helical insert. The swirl number $S_{N,f}$ [24] was defined as

$$S_{N,f} = \frac{\pi d_0 D_s \cos\varphi}{4nwl} \tag{2}$$

(its approximately value was 0.8). The air swirler shown in Fig. 2 was used to impart the swirl motion to the air flow. The approximate theoretical swirl number of this air swirler was calculated by the formula [17]

$$S_{N,a} = \frac{2}{3}\tan\theta, \tag{3}$$

where θ is the angle of the vanes with respect to the horizontal line (when the swirler is kept horizontally). This angle is also called the swirl angle. It was kept as 45° to obtain the swirl number $S_{N,a} \approx 0.67$ (approximately). Eight vanes 1.2 mm thick and 7.5 mm long were used to impart the swirl. The atomizer was placed at the center of this swirler with its outer diameter of 30 mm. The fuel tank was pressurized to 9 atm by using compressed air. The flow rate of the fuel was in the range of 56–107 ml/min. The range of the momentum flux ratios obtained by varying the amount of air was 353–966.

2. DIMENSIONLESS PARAMETERS

The following dimensionless parameters were used to obtain correlations among the flame height, fuel flow rate, and momentum flux ratio.

The power level ratio (P_r) of the fuel was defined as the ratio of the power level of the fuel at any particular flow rate to the power level of the fuel at the maximum flow rate used in the study:

$$P_r = \frac{G_f \rho_f Q}{G_{\max} \rho_f Q}, \tag{4}$$

where G_f is any particular flow rate of the fuel, $G_{\max}$ is the maximum flow rate of the fuel (in this study, 107 ml/min), ρ_f is the density of Jet A1 kerosene (807.5 kg/m^3), and Q is the calorific value of Jet A1 kerosene (43.1 MJ/kg).

The flame height ratio (H_r) was defined as the ratio of the flame height (H) to the exit orifice diameter of the pressure swirl atomizer used in the current study (d_0):

$$H_r = H/d_0. \tag{5}$$

In this work, the exit orifice diameter is $d_0 = 0.3$ mm. From here on, the "flame height" is understood as the flame height ratio.

The momentum flux ratio (MFR) is the ratio of the momentum flux of the fuel jet to the momentum flux of air discharged from the swirler normal to it:

$$\text{MFR} = \frac{\rho_f (v_f \sin\varphi)^2}{\rho_a (v_a \sin\theta)^2}, \tag{6}$$

where v_f and v_a are the average fuel and air velocities at the exit from the atomizer orifice and air swirler, respectively.

3. DESIGN OF EXPERIMENTS

In this study, we used the response surface methodology (RSM) [25, 26], which is an empirical statistical technique that uses the data obtained from a sequence of designed experiments for the regression analysis [27]. The RSM gives us the relationship between several independent variables (factors) and one or more dependent variables (response variables). The RSM was applied here with two design factors: the power level ratio and the momentum flux ratio. The flame height ratio was considered as a response variable. The design of experiment (DOE) technique used in this work is the D-optimal design. We chose this instead of central composite design (CCD), which is more often used, as we did not want to conduct experiments outside of the design space. To be robust, the CCD requires a few experiments outside the design space. DOE techniques are employed before, during, and after the regression analysis to evaluate the accuracy of the model.

The images of the flame height were obtained from a digital camera Casio Exilim EX-F1. By using this

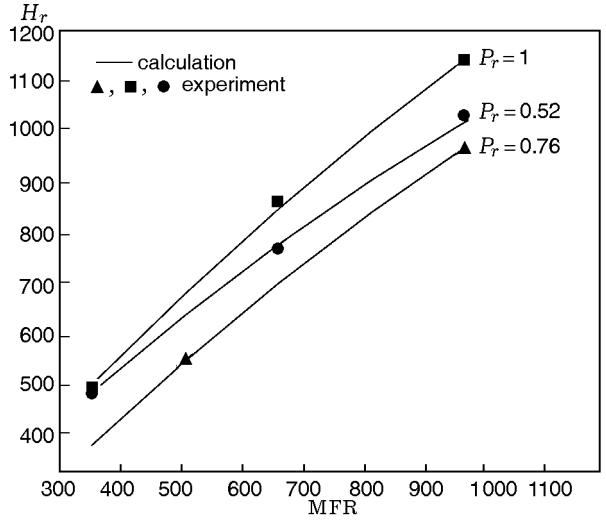

Fig. 3. Flame height ratio versus the momentum flux ratio for different fuel flow rates.

camera, videos of visible flames were obtained at 30 fps for different runs, which were converted into separate frames (images). The experiments were conducted in a completely dark room. The images were first converted into a binary form. Anything above 80 pixels of red, green, or blue was considered as a flame. The flame height measurements in pixels were carried out by using image processing techniques, such as smoothing, sharpening, and edge detection for exact identification of the flame tip with a MatLab code. The flame height in pixels was multiplied by a certain factor to obtain the actual flame height in a particular frame. The flame height data for each run were then averaged and the standard deviations were obtained to determine the associated random errors. The mean error associated with the flame heights was around 16% for the correlation purpose and around 10% for the blowout purpose.

4. RESULTS AND DISCUSSION

4.1. Variation of the Flame Height with the MFR

The flame height is one of the important parameters used for characterizing the diffusion flame. Figure 3 shows the flame height ratio as a function of the momentum flux ratio for different fuel flow rates. The flame height was found to increase with increasing MFR for all fuel flow rates. Note that the MFR was increased by keeping the fuel flow rate constant and decreasing the air flow rate. The decrease in the air flow rate starts shifting the flame toward the buoyancy-controlled domain. This was inferred on the basis of changes in the flame structure and an increase in the flame height. As the amount of air decreases, the fuel droplets are unable to find enough air for complete combustion at lower heights, and the fuel-rich condition prevails. In this fuel-rich condition, combustion depends on entrainment of atmospheric air to a large extent. As a result, the fuel droplets start escaping to greater heights, mix with air, and burn to form the flame. Thus, the visible flame height starts increasing with a decrease in the air flow rate, which is attributed to inadequate entrainment of air and mixing between the fuel and air.

4.2. Variation of the Flame Height with the Fuel Flow Rate

As is seen from Fig. 3, the flame height increases with increasing MFR for a particular power level ratio P_r. For a fixed MFR, variation of P_r helps in understanding the effect of the spray behavior on the flame. In this case, the overall equivalence ratio at the inlet can be considered as constant. Therefore, an increase in the power level ratio in this case simply means that there will be an increase in the fuel flow rate with an unchanged overall equivalence ratio. This variation in the fuel flow rate results in fine spray formation due to a higher momentum force and enhanced mixing with ambient air. The reason why the curve for $P_r = 0.76$ is below the curves for $P_r = 1.0$ and 0.52 in Fig. 3 can be explained with the help of the data presented in Fig. 4. It can be observed that the flame height ratio decreases to a minimum value and subsequently increases with an increase in the power level ratio for a fixed MFR value. This parabolic nature suggests that the flame heights for P_r 1.0 and 0.52 will be above the flame height for $P_r = 0.76$. Constant-MFR curves are found to be parabolic, i.e., the flame height first decreases for lower values of the power level ratio and then increases for higher values of P_r. This variation can be explained with the help of the experiments conducted by Reddy and Mishra [23] to determine the spray characteristics of the pressure swirl atomizer. Note that the experiments were conducted with water as a test fluid. However, as both water and kerosene are low-viscosity fluids, kerosene is expected to show almost similar spray characteristics.

As the fuel flow rate is initially increased, the Sauter mean diameter (SMD) of the fuel droplets starts decreasing and the cone angle of the spray starts increasing. This leads to better atomization and mixing at lower heights. As a result, the flame height decreases. As the fuel flow rate is further increased above a certain value, the SMD and the spray cone angle both start showing negligible changes [23, 24]. This increase in

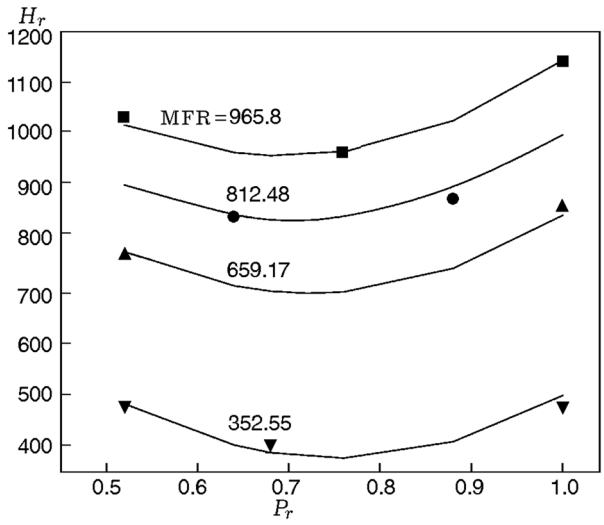

Fig. 4. Flame height ratio versus the power level ratio for different fixed momentum flux ratios: the points and curves show the experimental and numerical data, respectively.

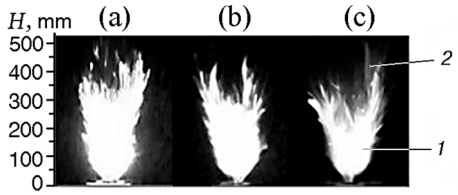

Fig. 5. Flame photographs for MFR = 352.55 and $P_r = 0.52$ (a), 0.68 (b), and 1 (c): (*1*) primary diffusion flame; (*2*) secondary premixed flame; the scale is ≈14.7 : 1.

the fuel flow rate starts increasing the momentum of fuel droplets. Despite better atomization, it leads to escaping of droplets from the primary flame. These fine droplets burn at the top of the primary flame giving a bluer region. The extent of the premixed flame increases with the fuel flow rate, which is evident from Fig. 5 (as an increase in the secondary blue flame).

As is seen from Fig. 5, for the $P_r = 0.52$ case, some of the fuel droplets burn at the top of the primary flame clearly due to poor atomization. However, as the fuel flow rate is increased, atomization improves, and no separate droplet burning at the top is observed for the $P_r = 0.68$ case. Thus, the flame height is smaller as compared to the $P_r = 0.52$ case. A blue region is visible in the $P_r = 1.0$ case, which accounts for better atomization and momentum-dominated nature of the flame. It is clear from Fig. 5c that a large number of fuel droplets escape and burn at the top of the primary flame in the presence of excess air. In this case, due to better atomization, separate burning droplets (as in the $P_r = 0.52$ case) are not visible, but a blue region prevails at the top of the primary flame. Thus, the flame height decreases slightly from the $P_r = 0.52$ case to a minimum value and subsequently increases for the same MFR. As is seen from Fig. 3, the flame height increases with increasing MFR for a fixed value of P_r.

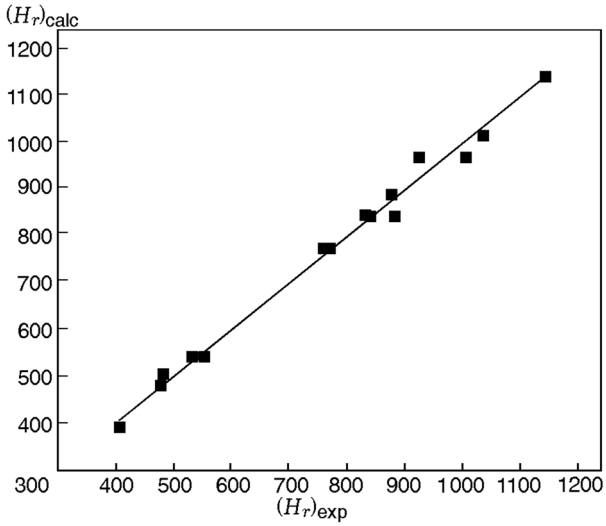

Fig. 6. Comparison of experimental data (points) with results predicted by Eq. (7) (straight line).

4.3. Correlation for the Flame Height Ratio

A design layout was prepared for carrying out the experiments to develop a correlation for the flame height ratio in terms of the power level ratio and momentum flux ratio. The RSM [25, 26] was applied with two design factors, and the flame height ratio was considered as a response variable.

The number of trials, which is based on the number of design factors, was 16 (11 combinations and 5 replications). This design layout made sure that the most accurate prediction could be generated with the least number of experiments being conducted. The design layout was obtained by using Design Expert, a specialized software system for preparing design layouts with the use of many design methods and for predicting the most accurate model based on the results of the design layout. The uncertainty in the predicted data in the present case ranged from 0.1 to 4.5% with a mean of 2%. The predicted and experimental data are compared in Fig. 6. They are found to be in good agreement. The resulting correlation

$$H_r = a - bP_r + c\mathrm{MFR} + dP_r\mathrm{MFR} + eP_r^2 - f\mathrm{MFR}^2 \quad (7)$$

was rigorously tested for other regions in the design space. Here $a = 1148.87012$, $b = 3061.481$, $c = 1.031$,

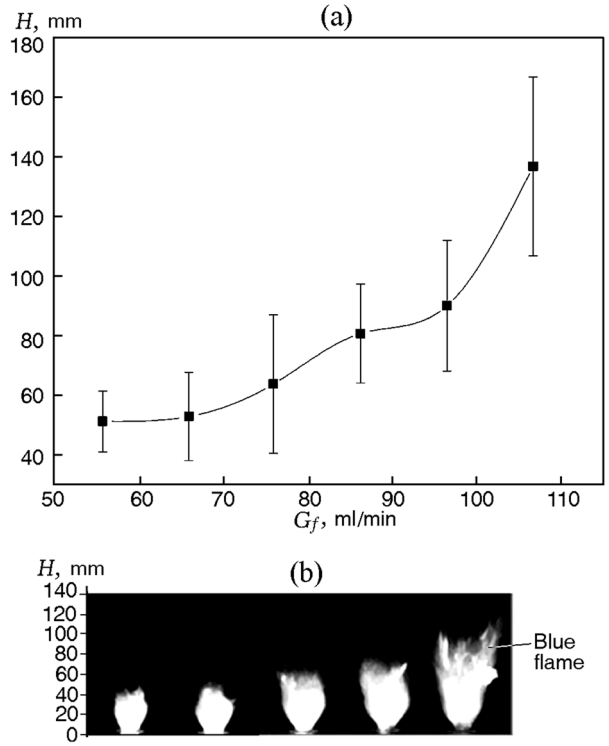

Fig. 7. (a) Flame height before the threshold lean blowout air velocity is reached versus the fuel flow rate. (b) Photographs of the corresponding flames for G_f = 56, 76, 86, 97, and 107 ml/min (from left to right; the scale is ≈14.8 : 1).

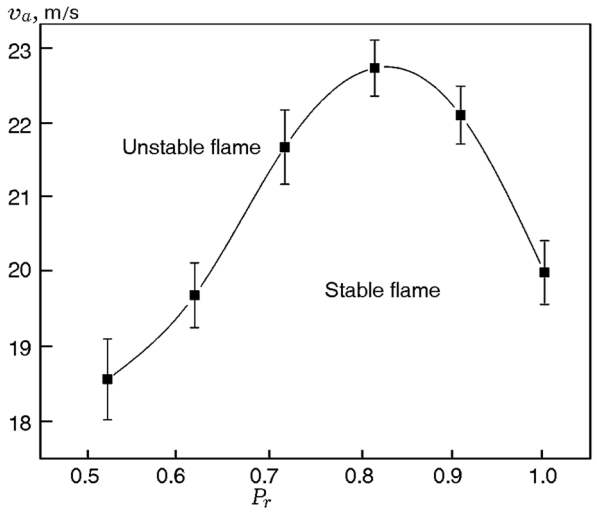

Fig. 8. Lean blowout air velocity versus the fuel flow rate.

$d = 0.36789$, $e = 1950.55740$, and $f = 2.63558 \cdot 10^{-4}$. Now, as Eq. (7) is a quadratic in both P_r and MFR, the curves for both variables should be parabolic. However, it is seen from Fig. 3 that the flame height varies almost linearly with the MFR. This is because the last coefficient f in the equation is very small. Therefore, the value of $f\text{MFR}^2$ is small as compared to the values of other terms in the equation and, hence, can be neglected. Thus, Eq. (7) can be considered as linear in terms of the MFR and parabolic in terms of P_r.

4.4. Lean Blowout Limit

The lean blowout limit can be defined as the threshold air velocity at which the flame can still remain stable for a particular fuel flow rate. The experiment was conducted by keeping the fuel flow rate constant and gradually increasing the air flow rate until the flame became unstable and blew off. A number of videos were taken to locate the transition between the stable and unstable flame and the variation of the flame height at the lean blowout velocity for different fuel flow rates.

The flame height was found to remain almost constant at low values of the fuel flow rate, but subsequently increased sharply with increasing fuel flow rate, as is shown in Fig. 7a. At low values of the fuel flow rate, the spray cone angle increases and the SMD of fuel droplets decreases with the fuel flow rate [23, 24], as discussed earlier. Thus, atomization and mixing start improving rapidly, and all the fuel droplets are consumed by air despite the increase in the fuel flow rate. However, it can be noted that there is only a slight increase in the flame height at low fuel flow rates (see Fig. 7a). For a similar reason, only a few fine droplets are found to escape the flame, representing a very small blue region above the flame, as is shown in Fig. 7b. However, at higher values of the fuel flow rate, a larger blue region starts appearing at the top of the flame, which indicates that the flame is located in the well-mixed region and, hence, is susceptible to blowout. It is seen from Fig. 7a that the flame height increases with the fuel flow rate. This increase in the flame height and the blue region can be due to the asymptotic behavior of the SMD and the spray cone angle at these fuel flow rates [23, 24], as explained earlier in Section 4.2. Thus, due to the increase in the fuel flow rate, the momentum of fuel droplets increases, leading to formation of a fine spray. Hence, the spray with a fine droplet distribution and a wider spray cone angle helps in enhancing mixing of the vaporized fuel and air, thus, providing a light blue region at the top. Note that the extent of the premixing flame is enhanced; thus, the lean blowout velocity starts decreasing.

The lean blowout limit v_a follows a parabolic trend as a function of P_r, as is shown in Fig. 8. It first increases with increasing fuel flow rate and then decreases. The low blowout limit at low fuel flow rates can be attributed to poor atomization. However, as the at-

omization starts improving with the fuel flow rate, the flame blows out at a higher air flow rate; thus, the lean blowout limit increases. However, above a certain fuel flow rate, the SMD and the spray cone angle become almost constant. A further increase in the fuel flow rate leads to an increase in the momentum of droplets and enables them to escape the flame kernel without burning (see Fig. 7b). An increase in the air flow rate in this situation results in quenching of the recirculation zone, eventually leading to lean blowout. Thus, at higher values of the fuel flow rate, the lean blowout velocity starts decreasing due to escaping of droplets from the flame kernel, leading to incomplete combustion. The average error in the calculation of the lean blowout limit was found to be ≈4%.

CONCLUSIONS

In this work, the spray flame of the kerosene-based Jet A1 fuel was characterized for different MFRs and fuel flow rates in terms of the visible flame height. The optimal design methodology was adopted for deriving an empirical relationship for the flame height ratio in terms of the MFR and power ratio, which can be used for design of kerosene-based combustion systems. The lean blowout limits were also investigated for different fuel flow rates. The results of the present experimental investigation can be summarized as follows.

• The flame height ratio was found to increase with increasing MFR at a constant fuel flow rate. The flame height first decreases to a minimum value with increasing power level ratio and subsequently starts increasing for all fixed MFR values. This behavior of the flame height ratio with the power level can be attributed to improvement of spray formation and to an increase in the extent of the premixed flame due to escaping of high-momentum droplets forming a secondary premixed flame zone above the primary diffusion flame region.

• An empirical relationship (7) of the flame height ratio with the power level and MFR was developed in a dimensionless form by using the response surface optimal design layout.

• The lean blowout limit follows a parabolic relationship with the fuel flow rate. It first increases with fuel flow rate to a maximum value with improvement of atomization and then starts decreasing with a further increase in the fuel flow rate. This parabolic relationship is attributed to improvement of spray formation and to an increase in the extent of the premixed flame region with an increase in the fuel flow rate.

REFERENCES

1. N. A. Chigier and M. F. Roett, "Twin-Fluid Atomizer Spray Combustion," in *ASME Winter Annual Meeting* (New York, 1972), Paper No. 79-WA/HT-25.
2. Y. Onuma and M. Ogasawara, "Studies on the Structure of a Spray Combustion Flame," in *Fifteenth Symp. (Int.) on Combustion* (The Combustion Inst., Pittsburgh, 1975), pp. 453–465.
3. A. M. Mellor, "Workshop on Combustion Measurements in Jet Propulsion Systems," Project SQUID (Purdue Univ., 1976).
4. J. E. Usowicz, "An Experimental Study of Flame Lengths and Emissions of Fully-Modulated Diffusion Flames," M. Sc. Thesis, (Worcester Polytechnic Inst., 2011).
5. H. A. Becker and D. Hang, "Visible Length of Vertical Free Turbulent Diffusion Flames," Combust. Flame **32**, 115–137 (1978).
6. T. R. Blake and M. McDonald, "An Examination of Flame Length Data from Vertical Turbulent Diffusion Flames," Combust. Flame **94**, 426–432 (1993).
7. T. R. Blake and J. B. Cote, "Mass Entrainment, Momentum Flux, and Length of Buoyant Turbulent Gas Diffusion Flames," Combust. Flame **117** (3), 589–599 (1999).
8. F. V. Bracco, "Nitric Oxide Formation in Droplet Diffusion Flames," in *Fourteenth Symp. (Int.) on Combustion* (The Combustion Inst., Pittsburgh, 1973), pp. 831–842.
9. A. Williams, "Combustion of Droplets of Liquid Fuels, a Review," Combust. Flame **21** (132), (1973).
10. A. M. Mellor, "Simplified Physical Model of Spray Combustion in a Gas Turbine Engine," Combust. Sci. Technol. **8**, 101–109 (1973).
11. S. K. Aggarwal and W. A. Sirignano, "Ignition of Fuel Sprays Deterministic Calculations for Idealized Droplet Arrays," in *Twentieth Symp. (Int.) on Combustion* (The Combustion Inst., Pittsburgh, 1984), pp. 1773–1780.
12. D. Feikema, R. H. Chen, and J. F. Driscoll, "Enhancement of Flame Blowout Limits by the Use of Swirl," Combust. Flame **80**, 183–195 (1990).
13. D. Feikema, R. H. Chen, and J. F. Driscoll, "Blowout of Nonpremixed Flames: Maximum Coaxial Air Velocities Achievable, with and without Swirl," Combust. Flame **86**, 347–358 (1991).
14. R. H. Chen, J. F. Driscoll, J. Kelly, M. Namazian, and R. W. Schefer, "A Comparison of Bluff Body and Swirl Stabilized Flames," Combust. Sci. Technol. **71**, 197–217 (1990).
15. N. Syred and J. M. Beer, "Combustion in Swirling Flows: A Review," Combust. Flame **23**, 143–201 (1974).
16. J. M. Beer and N. A. Chigier, *Combustion Aerodynamics* (Appl. Sci. Publ., London, 1972).
17. A. H. Lefevbre, *Gas Turbine Combustion* (Taylor and Francis, 1998).

18. Weiland N., Chen R. H., and Strakey P. "Effects of Coaxial Air on Nitrogen-Diluted Hydrogen Jet Diffusion Flame Length and NO_x Emission," Proc. Combust. Inst. **33** (2), 2983–2989 (2011).
19. M. A. Delichatsios, "Transition from Momentum to Buoyancy-Controlled Turbulent Jet Diffusion Flames and Flame Height Relationships," Combust. Flame **92**, 349–364 (1993).
20. J. S. Shuen, "Prediction of the Structure of Fuel Sprays in Cylindrical Combustion Chambers," J. Propul. Power **3** (2) (1987).
21. V. H. Morcos and Y. M. Abdel-Rahim, "Parametric Study of Flame Length Characteristics in Straight and Swirl Light-Fuel Oil Burners," Fuel **78**, 979–985 (1999).
22. M. Nakamura, D. Nishioka, J. Hayashi, and F. Akamatsu, "Soot Formation, Spray Characteristics, and Structure of Jet Spray Flames under High Pressure," Combust. Flame **158**, 1615–1623 (2011).
23. K. U. Reddy and D. P. Mishra, "Studies on Spray Behavior of a Pressure Swirl Atomizer in Transition Regime," J. Propul. Power **24** (1), 74–80 (2008).
24. S. K. Chen, A. H. Lefebvre, and J. Rollbuhler, "Factors Influencing the Effective Spray Cone Angle of Pressure Swirl Atomizers," J. Eng. Gas Turb. Power **114**, 97–103 (1992).
25. S. Z. Abghari, J. Towfighi, R. Karimzadeh, and M. Omidkhah, "Application of Response Surface Methodology in Study of the Product Yield Distribution of Thermal Cracking of Atmospheric Gasoil," Scientia Iranica **15** (4), 457–468.
26. L. Davies, *Efficiency in Research Development, and Production: The Statistical Design and Analysis of Chemical Experiments* (The Roy. Soc. Chem., 1993).
27. M. Rajasimman and K. Murugaiyan, "Sorption of Nickel by Hypnea Valentiae: Application of Response Surface Methodology," Int. J. Civil Environ. Eng. **3** (1), (2011).